Available online at www.sciencedirect.com
SCIENCE DIRECT®
Pergamon
Cement and Concrete Research 34 (2004) 695–702
CEMENT AND CONCRETE RESEARCH

Corrosion resistance and chloride diffusivity of volcanic ash blended cement mortar

K.M.A. Hossain*, M. Lachemi

Department of Civil Engineering, Ryerson University, 350 Victoria Street, Toronto, ON, Canada M5B 2K3

Received 17 December 2002; accepted 27 October 2003

Abstract

This article reports the results of an investigation on the chloride diffusivity and corrosion resistance of volcanic ash (VA) blended cement mortars with varying curing times of up to 1 year. The mortars had 20% and 40% VA as cement replacement and water/binder ratio of 0.55. The accelerated chloride ion diffusion (ACID) test was used to calculate the chloride ion (Cl^-) diffusion coefficient (D_i) of the mortars using the Nernst–Plank equation for steady state condition. In addition, electrical resistivity, mercury intrusion porosimetry and differential scanning calorimetry (DSC) tests were conducted. Electrochemical measurement such as linear polarization resistance was used to monitor the corrosive behavior of the embedded steel bars. The chloride ingress into the mortars was also studied. Good correlations were found among D_i, total pore volume (TPV) and electrical resistivity of the mortars. It was also found that blending cement with VA significantly reduced the long-term D_i and hence increased the long-term corrosion resistance of mortars. This fact was also supported by the presence of lower quantity of $Ca(OH)_2$ and higher quantity of Friedel's salt in the VA blended mortars as observed from the DSC tests. Mortars with 40% VA showed better performance in terms of Cl^- diffusivity, chloride ingress and passivation period of embedded steel compared with the control mortar with 0% VA.

Keywords: Volcanic ash; Chloride ion diffusion; Pore volume; Electrical resistivity; Differential scanning calorimetry; Steel corrosion; Blended cement mortar

1. Introduction

The search for alternative binders or cement replacement materials had been continued for the last decades. Research had been carried out [1–8] on the use of volcanic ash (VA), volcanic pumice (VP), fly ash (FA), pulverized-fuel ash (PFA), blast furnace slag, rice husk ash, silica fume, etc., as cement replacement material. The VA, VP, PFA and FA are pozzolanic materials because of their reaction with lime ($Ca(OH)_2$) liberated during the hydration of cement. Amorphous silica present in the pozzolanic materials combines with lime and forms cementitious materials. These materials can also improve the durability of concrete and rate of gain in strength and reduce the rate of liberation of heat, which is beneficial for mass concrete. The reactivity of FA has been found to depend on the mineral substitution in the glassy silica structure. FAs containing high amounts of calcium oxide have both cementing and pozzolanic activities while those containing mainly aluminum oxide and iron oxide as the major minerals substituted in the structure of the silica glass only have pozzolanic activity. Studies had been published concerning the effect of FA on concrete porosity and resistivity [9], pore solution chemistry [10], oxygen and chloride ion (Cl^-) diffusivity [9–13], carbonation rates [14], passivation [15] and corrosion resistance [16], especially chloride-induced corrosion.

Comprehensive research had been conducted over the last few years [1,17–19] on the use of VA and VP in cement and concrete production. The meaningful use of such volcanic debris can transform them into natural resources and not only can provide low-cost cement and concrete but also can help to decrease environmental hazard in volcanic areas of the world. Research results suggest that the manufacture [1] of blended Portland VA cement (PVAC) and Portland VP cement (PVPC) similar to Type C Portland cement and Type FC Portland FA cement (PFAC) is possible with maximum replacement of up to 20%.

* Corresponding author. Tel.: +1-416-979-5000x7867; fax: +1-416-979-5122.
E-mail address: ahossain@ryerson.ca (K.M.A. Hossain).

0008-8846/$ – see front matter © 2004 Elsevier Ltd. All rights reserved.
doi:10.1016/j.cemconres.2003.10.021

Durability of concrete is one of its most important desirable properties and it is essential that the concrete made with VA and VP blended cement should be capable of preserving its durability throughout the life of structures. Until recently [20], little research had been conducted on the degradation of VA blended cement concrete subjected to aggressive environment. The problem of corrosion of steel in concrete is very important. The diffusion of Cl^- through concrete is a major cause of corrosion of reinforcing bars in offshore structures as well as highway bridges in cold countries where deicing salts (NaCl and $CaCl_2$) are used during the winter.

The diffusivity of chloride through concrete depends on the microstructure of the concrete/mortar. Blending cement with cementitious materials like FA is known to produce mortar/concrete with a dense microstructure [21] and hence an improvement in the physical protection of any embedded bars. In addition to this, if there were chloride binding by the aluminate phase to form Friedel's salt, then the concentration of the free Cl^- in the pore water of concrete/mortar would be expected to decrease. Currently, information is not available on the chloride binding or corrosion inhibition characteristics in VA blended cement mortar/concrete.

This article describes the Cl^- diffusivity of VA blended Portland cement mortars. It also presents the chloride binding ability of VA to form Friedel's salt. The beneficial effect of VA on the Cl^- diffusivity and corrosion inhibition is vital for the use of VA blended cement in concrete construction subjected to marine environment or deicing salt.

2. Experimental investigation

2.1. Materials and mix proportions

The VA used in this investigation was collected from the Rabaul area of the East New Britain province of Papua New Guinea and the source was a volcano called Mount Tavurvur. The Rabaul area is situated in the worldwide earthquake and volcanic zone known as the "belt of fire." The cement used was locally manufactured ordinary Portland cement (OPC) called "Paradise" conforming to ASTM Type I. Ordinary drinking water was used in the mortar mixes.

Chemical and physical properties of VA are compared with those of Paradise cement in Table 1. VA is principally composed of silica (about 60%) while the main component of cement is calcium oxide (maximum 70%). VA also has compounds like calcium oxide, alumina and iron oxide (total about 31%). The Blaine fineness and oven dry bulk density of VA are 285 and 2450 kg/m^3, respectively. VA satisfies the requirement of Class F FA as per ASTM C618 [22]. The Portland cement has a specific gravity of 3.15 and Blaine fineness of 320 m^2/g.

River sand of fineness modulus 2.40 having a specific gravity of 2.65 and water absorption of 0.6% was used.

Table 1
Chemical and physical properties of cementing materials

Chemical compounds	VA (%)	Paradise cement (Type I) (%)
Calcium oxide (CaO)	6.1	64.1
Silica (SiO_2)	59.3	21.4
Alumina (Al_2O_3)	17.5	5.7
Iron oxide (Fe_2O_3)	7.0	3.5
Sulfur trioxide (SO_3)	0.7	2.1
Magnesia (MgO)	2.6	2.1
Sodium oxide (Na_2O)	3.8	0.5
Loss on ignition	1.0	1.1
Fineness (m^2/kg)	285	320

These materials were used to prepare the mortar mixes with water/(cement + VA) ratio of 0.55. VA replacement of 20% and 40% by weight were used in the mortar mixes. In addition, control specimens were prepared without VA (0%). Table 2 shows the mixture proportions of the mortars.

Cylindrical specimens 100 mm in diameter and 200 mm in height, 50 mm in diameter and 100 mm in height, 70 mm cubes and 180 × 100 × 70 mm mortar blocks with steel bars were cast to carry out the tests.

2.2. Experimental methods

2.2.1. Accelerated chloride ion diffusion (ACID) test on mortar

The ACID test [23–25], an improvement over the rapid chloride permeability test (AASHTO T277) [26], was used to determine the Cl^- diffusion coefficient (D_i) of mortars. In this test, a diffusion cell (volume 785 ml) using 3% NaCl and 0.3 N NaOH as cathode and anode solutions, respectively, was used. The tests were conducted at 7, 28, 91 and 180 days of moist curing of the specimens. Mortar specimen (100 mm in diameter × 20 mm thick) was placed between the electrodes and an electric field of 3 V/cm was applied to the electrodes. The amount of Cl^- that migrated from the cathode through the mortar specimen to the anode of the cell was determined by measuring the concentration of the Cl^- in the anode solution periodically. The amount of Cl^- versus time (days) gives a straight line and the slope of this straight line is termed as Cl^- flux (f_i). f_i was used in the Nernst–Plank equation (Eq. (1)) to calculate the chloride D_i [23,24]:

$$D_i = \frac{RTf_i}{I_c F C_i \delta V} \quad (1)$$

where D_i (cm^2/s), R = universal gas constant (8.314 J/K mol), T = temperature (K), I_c = ionic charge of Cl^-, F = Faraday constant (9.65 × 10^4 C/mol), C_i = Cl^- concentration in the anode chamber of the diffusion cell and δV = electric field (V/cm).

2.2.2. Electrical resistivity of mortar

The electrical resistivity was measured with an automatic LCR meter by applying a 10-mV AC at 1 kHz

Table 2
Mortar mix proportions

Specimen	Water/ (cement + VA)	Water (kg/m^3)	Cement (kg/m^3)	VA (kg/m^3)	Sand (kg/m^3)
0% VA (control)	0.55	385	700	0	2100
20% VA	0.55	385	560	140	2100
40% VA	0.55	385	420	280	2100

across saturated specimens (50 mm in diameter × 50mm thick) using copper plate electrodes. The instrument gave a digital display of the value of the electrical resistance. The value of the resistance measured was then used to calculate the electrical resistivity. The tests were conducted at 7, 28, 91 and 180 days of moist curing of the mortar specimens.

2.2.3. Total pore volume (TPV) of mortar

The mercury intrusion porosimetry was used to measure the TPV of the cement and cement-VA mortars. The tests were conducted at 7, 28, 91 and 180 days of moist curing of the mortar specimens.

2.2.4. Compressive strength of mortar

The tests were conducted at 7, 28, 91 and 180 days of moist curing of the 70-mm mortar cubes to evaluate their compressive strength.

2.2.5. Chloride concentration profiling

Cylindrical mortar specimens of 50 mm in diameter and 100 mm high were used. After demoulding, the mortar specimens were cured for 7 and 28 days in a moist environment. After curing for a prescribed time, the sides and top surface of the specimens were coated with the epoxy resin, leaving the bottom surface uncoated to simulate a one-dimensional diffusion. The specimens were then kept in an environmental chamber. While in the chamber, the specimens were sprayed with a 5% NaCl solution every 3 days. A temperature and relative humidity of 20–25 °C and 70–80%, respectively, were maintained during exposure. After an exposure period of 365 days, the specimens were removed from the chamber. A specimen was sliced into five discs of thickness 10 mm. These were then ground into fine powder passing the 150-μm sieve. The total chloride contents were then measured [27]. A 2 M HNO_3 solution was added to the powder, and the mixture was titrated with 0.005 M $AgNO_3$ solution to determine the total chloride content of the mortar powder. The results were used to plot graphs of the chloride content versus depth from the surface of the specimen.

2.2.6. Corrosion monitoring and differential scanning calorimetry (DSC)

Mortar blocks having dimensions of 180 × 100 × 70 mm were used. Two commercial mild steel bars with 10 mm in diameter, polished with emery paper, were embedded in each block, with a cover thickness of 20 mm. External stainless steel plugs were connected to one end of the steel bars to serve as contact points for electrical connection. The blocks were cured for 28 days in a moist environment. After curing, specimens were placed in the environmental chamber. The specimens in the chamber were sprayed with a 5% NaCl solution every 3 days.

The corrosion process of steel in concrete can be followed using several electrochemical techniques. Monitoring of open circuit potential (OCP) is the most typical procedure to the routine inspection of reinforced concrete structures [28]. Its use and interpretation are described in the ASTM Standard Test Method for Half-Cell Potentials of Uncoated Reinforcing Steel in Concrete [29]. The OCPs of steel bars were monitored up to 180 days using a high impedance voltmeter and noting the potentials against a saturated calomel electrode (SCE).

At the end of corrosion monitoring test, the mortar specimens were split open, and the steel bars were carefully removed from the embedded mortar blocks. Their corroded areas were measured. The rust on the steel bars was then removed by immersion in 10% di-ammonium hydrogen citrate solution at a temperature of 50 °C for 24 h. After removal, they were cleaned to remove all rust and weighed to determine their weight loss resulting from the corrosion.

The DSC test was performed on mortar samples taken from portions around the steel bars to determine the quantity of Friedel's salt and $Ca(OH)_2$ formed in mortars.

3. Test results

3.1. Cl^- D_i

Fig. 1 shows the variation of D_i with curing time and with different %VA. The D_i decreased with the increase of

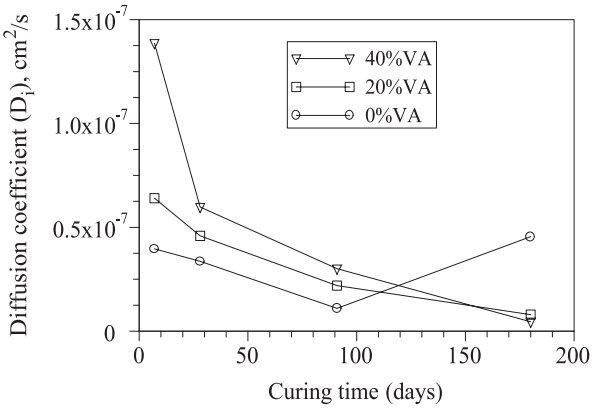

Fig. 1. Variation of D_i with curing time and %VA.

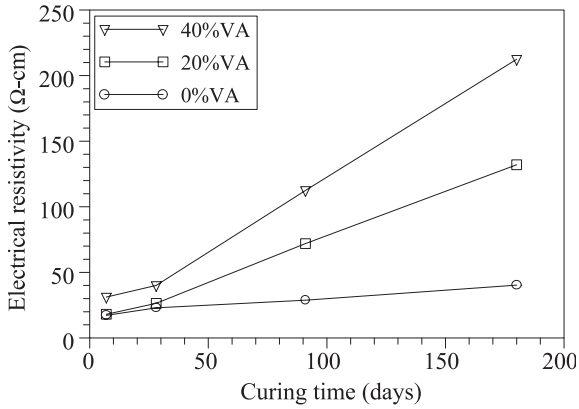

Fig. 2. Variation of electrical resistivity with curing time and %VA.

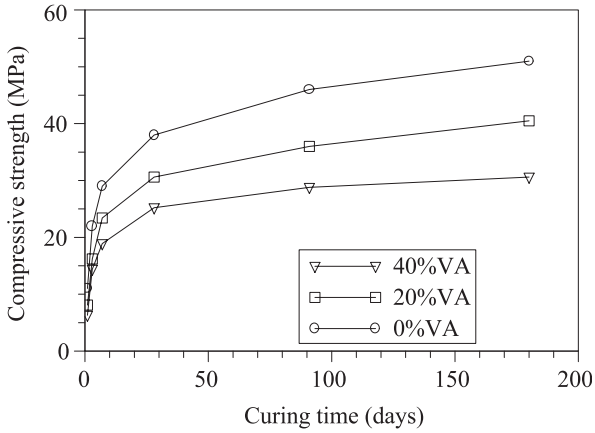

Fig. 4. Compressive strength as a function of curing time and VA content.

curing time for cement-VA mortars. The D_i of control mortar (0% VA) decreased with the increase of curing time for up to about 100 days. After 100 days, D_i of such mortar was found to increase with the increase of curing time and showed higher values compared with VA blended cement mortars. This can be attributed to the beneficial effect of VA on the long-term chloride diffusivity of VA blended cement mortars. The long-term beneficial effect on chloride diffusivity was found to be slightly better in 40% VA mortar than 20% VA mortar.

3.2. Electrical resistivity

Fig. 2 shows the variation of electrical resistivity with curing time and %VA. The electrical resistivity of the cement-VA mortars increased rapidly with the curing time. The 40% VA mortars had shown substantially higher resistivity than 20% VA mortars. On the other hand, the resistivity of the control mortar (0% VA) did not increase with the curing time especially in the long-term and remained lower than the VA mortars. Electrical current through hydrating cement mortar is electrolytic (i.e., mainly due to the flow of ions through the pore spaces). Hence, the electrical resistivity is an indirect measurement of porosity and diffusivity [30]. In reinforced concrete structures at the onset of corrosion of the bars, the corrosion current and hence the rate of corrosion is influenced by the electrical resistivity of the concrete. The high electrical resistivity of VA blended cement mortars would enhance the overall resistivity of VA blended concrete and hence a lower rate of bar corrosion after the breakdown of passivity.

3.3. TPV

The TPV decreased with the increase of curing time (Fig. 3). The increase of VA contents increased TPV. Mortar specimens with 40% VA showed higher TPV than the specimens with 0% and 20% VA.

3.4. Compressive strength

Fig. 4 shows the variation of compressive strength of mortar specimens with curing time and %VA. The rate of

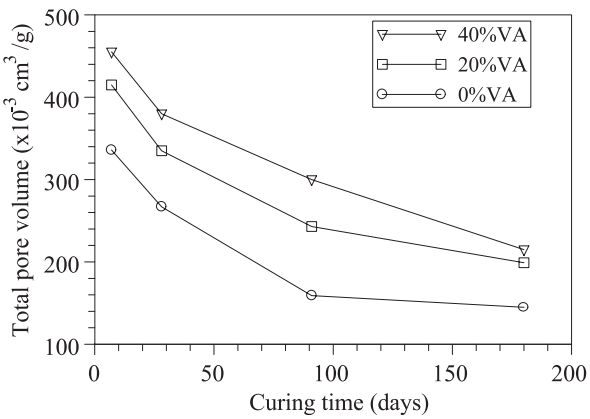

Fig. 3. TPV as a function of curing time and VA content.

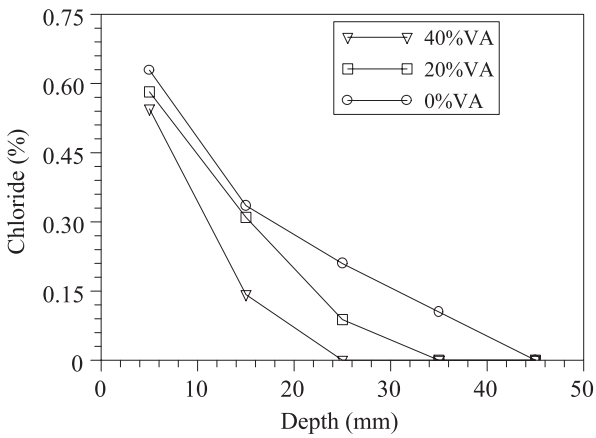

Fig. 5. Chloride concentration profile (7-day cured specimens).

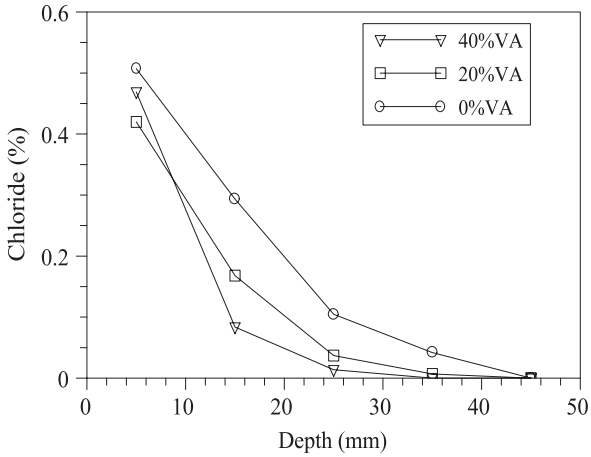

Fig. 6. Chloride concentration profile (28-day cured specimens).

strength development of the VA blended cement mortars was slower compared with that of the control specimens (0% VA). This indicated that the presence of VA retarded the setting process similar to that observed in FA [31]. The compressive strength was also decreased with the increase of VA.

3.5. Chloride ingress

Figs. 5 and 6 show the chloride concentration profiles of the mortar specimens at 365 days of exposure. The chloride content at different depths decreased with the increase of VA content. For both sets of specimens moist cured for 7 and 28 days before exposure to the 5% NaCl environment, the addition of VA to the cement resulted in a reduction in chloride ingress significantly beyond the depth of 25 mm compared with the control mortars with 0% VA. The chloride ingress in 7-day precured specimens (Fig. 5) was higher compared with the 28-day precured specimens (Fig. 6). The 40% cement replacement resulted in the lowest chloride ingress at deeper depths in both sets of specimens.

Table 3
DSC and corrosion test results

Specimen	28-day precured, 365 days curing time		$Ca(OH)_2$	Friedel's salts
	Weight loss (%)	Corroded area (%)	(J/g)	(J/g)
0% VA (control)	0.61	9.1	111	10
20% VA	0.42	6.2	58	16
40% VA	0.12	5.1	23	35

3.6. Corrosion resistance

Fig. 7 shows the variation of OCP of the steel bars in the mortar blocks with age. The potential time curves were used to evaluate the time to initiation of rebar corrosion based on ASTM C876 [29] criterion of −270 mV SCE. Immediately after exposure, the potential readings were in the range 0 to −180 mV, revealing a passive state. After a period that was dependent on the VA content, all the specimens showed potential decay toward more negative values, revealing the initiation of the corrosion process. The specimens with higher VA content showed less negative potentials than the specimens without VA. Specimens with 0% VA remained passive for about 2 weeks, whereas the specimens with 20% and 40% VA remained passive for about 6–7 weeks. The time for activation increased with the increase of VA content in the mortar. Mortar blocks with 40% VA showed better corrosion resistance.

Table 3 shows the weight loss and corroded area of steel bars obtained from the physical measurements. The weight losses and corroded area of steel bars embedded in the VA blended specimens were lower than those of control specimen (0% VA). Bars in 40% VA mortar specimens showed

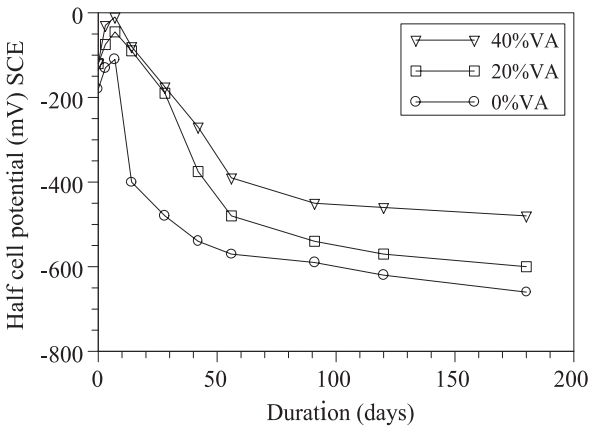

Fig. 7. OCP development in mortar specimens.

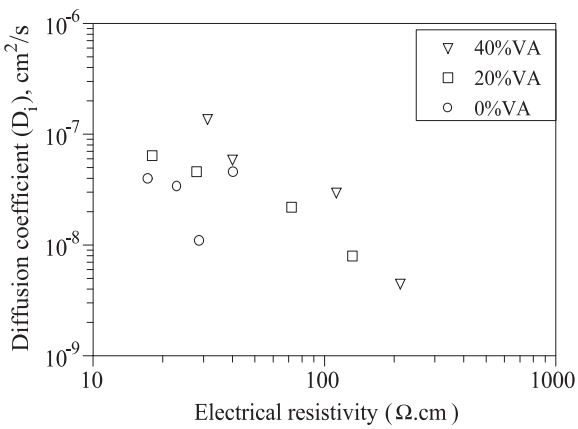

Fig. 8. Logarithmic correlation between D_i and electrical resistivity.

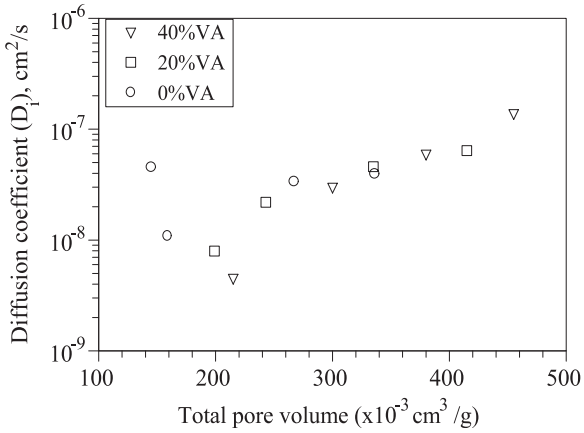

Fig. 9. Scatter diagrams of D_i versus TPV.

lowest corrosion with the lowest weight loss of only 0.12% and lowest corroded area of 5.1%.

4. Correlation among various parameters

Fig. 8 shows a logarithmic scatter diagram of D_i and electrical resistivity of the mortars. It shows a good correlation between D_i and electrical resistivity, with D_i being inversely proportional to electrical resistivity. This means that D_i of Cl^- through cement mortars could be derived from the value of its electrical resistivity [32]. Because electrical resistivity measurement is simple and nondestructive, such a relation would be very useful for researchers in this field.

Fig. 9 shows the scatter diagrams of D_i plotted on a log scale versus TPV plotted on a normal scale. It is observed that there is a correlation between D_i and TPV. The general trend shows an increase in D_i with the increase of TPV in the mortars.

Fig. 10 shows the scatter diagrams showing the relationship between logarithm of electrical resistivity and TPV of the mortars plotted on normal scale. It is seen that there is a correlation and the logarithm of the electrical resistivity is inversely proportional to the TPV. However, for a constant TPV, the electrical resistivity of the mortars is found to increase with the increase of VA content.

5. Discussion

Table 3 shows the results of DSC for the mortars at a curing age of 365 days. DSC thermograms show peaks due to endothermic (heat absorbing) and exothermic (heat releasing) reactions. The $Ca(OH)_2$ and Friedel's salt contents are equivalent to the area (enthalpy) under the respective endothermic peaks. The endothermic peak for $Ca(OH)_2$ was observed at around 450 °C. The quantity of $Ca(OH)_2$ formed in the hydration of the mortar decreased with the addition of VA (Table 3). Lowering of $Ca(OH)_2$ also indicated that the pozzolanic reactivity of the VA consumed $Ca(OH)_2$ resulting from the hydration of the cement. Such a pozzolanic [20] reaction of VA with $Ca(OH)_2$ produced a denser mortar and thus inhibited the ingress of Cl^-. This improved the corrosion resistance of VA blended cement mortar compared with OPC mortar (0% VA). This was justified from the long-term lower value of D_i (Fig. 1), higher electrical resistivity (Fig. 2) and lower chloride ingress at deeper depth (Figs. 5 and 6) in VA blended mortar specimens compared with control (0% VA) mortar specimens as observed in the current study.

VA was added as fine granulates, and on hydration, it had the capability of partially obstructing voids and pores. This lead to a decrease of pore size with refinement of pore structure (Fig. 11) and to a smaller effective diffusivity for chloride or other species (Fig. 1) as confirmed from the experimental results. The effect of VP on the pore size distribution within the TPV for pore sizes <20 nm (micropores) and pore sizes >20 nm (macropores) at different curing times is presented in Fig. 11. Fig. 11 plotted the percentage of TPV <20 or >20 nm against the curing time. It was noted that increasing levels of replacement of cement

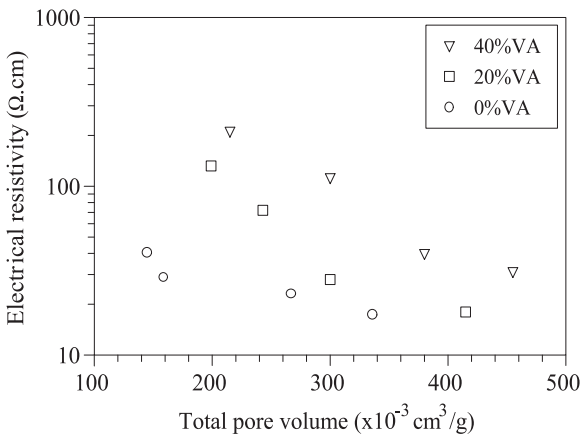

Fig. 10. Relationship between electrical resistivity and TPV.

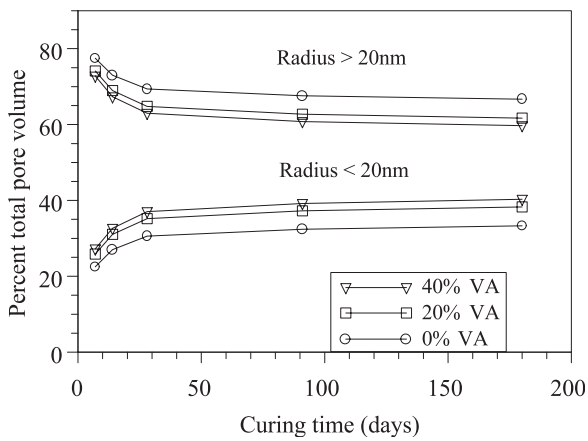

Fig. 11. Pore size distribution with curing time.

with VA (up to 40%) produced a refinement of pore structure of the mortar. This would improve the long-term corrosion resistance of VA-based concrete structures.

The presence of VA also affected the composition and thickness of the passive films. The thickening of the passive films due to the presence of VA was confirmed from the lowering of corrosion area of steel bars (Table 3). The corrosion area of steel bar reflects the extent of destruction of passive film by chloride. However, the corrosion rate, in other words, oxidation reaction rate, is also controlled by the amount of oxygen gas supply through cover concrete. Films formed in paste solutions have revealed a thickening and a higher degree of hydration under the influence of FA [15].

The presence of VA can strongly affect the chloride profile. Usually, chlorides penetrate in concrete by diffusion along water paths or open pores. Part of these chlorides can react with the cement hydration products, mainly tricalciumaluminates (C_3A), forming stable chlorocomplexes. The excess of chloride is free and leads to the initiation of the corrosion process. The presence of VA can lead to an increase of the amount of C_3A due to the higher amount of alumina present in the mix and to an increase of the content of calcium silicate hydrate that is formed in the pozzolanic reactions. Thus, the binding capacity of the concrete to chloride tends to increase, and consequently, less free chloride will be available to initiate the corrosion process [33].

The DSC analysis indicated the presence of Friedel's salts ($C_3A{\cdot}CaCl_2{\cdot}10H_2O$) as an endothermic peak at around 300 °C. Table 3 shows that the quantity of Friedel's salt increased with the addition of VA. This can be attributed to the fact that VA may have more amount of reactive alumina, which can adsorb more Cl^- to form Friedel's salts (C_3A content of VA was not measured in the current study). Friedel's salt formation consequently lowers the levels of free chloride and hence reduces the Cl^- diffusivity of concrete. This process can reduce the localized corrosion of embedded steel in such mortar. Comparatively higher Friedel's salt formation in VA blended cement mortar compared with control (OPC) mortar (0% VA) was confirmed from DSC test results (Table 3). The reduction in localized corrosion of embedded steel in VA blended cement mortar was confirmed from the lower weight loss and lower corroded area of steel bars in the current study (Table 3). Similar phenomena were also observed in FA concrete [33].

Hence, if bars are embedded in VA blended cement mortar, their passivation period based on $[Cl^-]/[OH^-]$ would be expected to decrease. Due to the decrease in the OH^- concentration or pH of the pore solution in the VA blended mortar, the passivity period of embedded bars would be longer compared with that in control (OPC) mortar [34]. This means that blending cement with VA would decrease the diffusivity of chloride through the resulting mortar, thereby increasing the passivation period of embedded bars. This phenomenon was observed in the current study where passivation period was increased in VA blended mortar specimens (Fig. 7). The overall effect of blending OPC with VA is, therefore, to prolong the passivation period of embedded bars in comparison with OPC and to improve the long-term corrosion resistance. Such beneficial effect of VA can be attributed to the refinement of pore structure, lowering of the presence of free chloride due to Friedel's salt formation and pozzolanic action.

6. Conclusions

This article presented the chloride diffusivity and corrosion resistance of VA blended cement mortar specimens with varying percentages of VA and curing time. The following conclusions were drawn from various tests conducted in this study:

(1) The Cl^- D_i decreased with the increase of the curing time but significant reduction only occurred at the later ages of curing. The control (OPC) mortar (0% VA) showed the development of higher D_i with time especially after 100 days in contrast to the decrease of D_i with the increase of curing time in VA blended cement mortars. The long-term beneficial effect on chloride diffusivity was found to be better in mortars with higher percentages of VA. Mortars with 40% VA produced slightly better results than 20% VA mortars.

(2) The 40% VA mortars had shown substantially higher electrical resistivity than 20% VA mortars. The high electrical resistivity of VA blended mortars would enhance the overall resistivity of VA blended concretes and hence could induce a lower rate of bar corrosion after the breakdown of passivity.

(3) ACID test method predicted D_i of mortar quite reasonably. Correlations are found between D_i and electrical resistivity as well as between logarithm of electrical resistivity and TPV. A correlation between electrical resistivity and TPV of the mortars is also established. The logarithm of the electrical resistivity is inversely proportional to TPV. The electrical resistivity of cement mortars can be used to predict D_i to make the measurement very simple and to make the nature of the test nondestructive.

(4) The incorporation of VA in mortar lead to refinement of the pore structure. The proportion of pores with radii smaller than 20 nm was increased as the replacement level of cement by VA increased. TPV also found to decrease with the increase of the curing time.

(5) VA blended specimens showed better resistance to chloride ingress, with 40% VA mortars exhibiting the lowest chloride ingress at deeper depths. The passivation period for the corrosion of steel bar was also increased in VA blended mortars. Bars in 40% VA mortar specimens showed the lowest weight loss of only 0.12% and lowest corroded area of 5.1% in embedded steel.

(6) DSC tests confirmed the formation of higher Friedel's salt and the presence of lower quantity of $Ca(OH)_2$ in VA mortar compared with OPC mortar (0% VA). Friedel's salt formation consequently lowered the levels of free chloride and the presence of lower $Ca(OH)_2$ was an indication of the pozzolanic reaction of VA with $Ca(OH)_2$ that produced a denser mortar. These phenomena improved the Cl^- diffusivity and hence lead to the higher corrosion resistance of VA blended mortar compared with OPC mortar (0% VA).

Acknowledgements

The authors thank the technical staff of the Materials Laboratory of the Department of Civil Engineering of the Papua New Guinea University of Technology for initial testing and preparation of the specimens and Tradescan Private, Bangladesh for providing generous voluntary financial assistance and for the successful completion of the tests.

References

[1] K.M.A. Hossain, Volcanic ash and pumice based blended cement, Proceedings of 23rd Conference on Our World in Concrete and Structures Incorporating 3rd International Seminar on Blended Cements, Singapore, 24 August, CI-Premier. Pte. Ltd., Singapore, 1998, pp. 297–302.
[2] K.M.A. Hossain, Volcanic ash as cement replacement material, Proceedings of the IEPNG International Conference, September 25–27, Rabaul, University of Technology Press, Lae, Papua New Guinea, 1998, pp. 31–37.
[3] M. Al-Ani, B. Hughes, Pulverized-fuel ash and its uses in concrete, Mag. Concr. Res. 41 (147) (1989) 55–63.
[4] P.K. Mehta, Properties of blended cements made from rice husk ash, J. ACI, (74) (1979) 440–442.
[5] R.N. Swamy, New Concrete Materials, Concrete Technology and Design, vol. 1, Surrey Univ. Press, Great Britain, 1983, p. 180.
[6] R.N. Swamy, Cement Replacement Materials, Concrete Technology and Design, vol. 3, Surrey Univ. Press, Great Britain, 1986, p. 272.
[7] E.E. Berry, V.M. Malhotra, Fly ash for use in concrete—A critical review, J. ACI 77 (8) (1980) 59–73.
[8] A. Bilodeau, V.M. Malhotra, High volume fly ash system: The concrete solution for sustainable development, Second CANMET/ACI Symposium on Sustainable Development of the Cement and Concrete Industry, October 21–23, Ottawa, 1998, pp. 193–214.
[9] M.D.A. Thomas, J.D. Matthews, Chloride penetration and reinforced corrosion in marine exposed fly ash concretes, in: V.M. Malhotra (Ed.), Proceedings of 3rd CANMET/ACI International Conference on Concrete in Marine Environment, ACI, Detroit, 1996, pp. 317–338 (ACI SP-163).
[10] C.M. Preece, F.O. Gronvold, T. Frolund, Corrosion of reinforcement in concrete construction, in: A. Crane, P. Crane (Eds.), Halstel, London, UK, 1983, p. 393.
[11] S.H. Lin, Calculation of seawater pH at polarized metal surfaces in the presence of surface films, Corrosion 46 (1990) 964.
[12] P.S. Mangat, K. Gurusamy, Chloride diffusion in steel fibre reinforced concrete, Cem. Concr. Res., (17) (1987) 385–396.
[13] M.M. Salta, in: R.N. Swamy (Ed.), Corrosion and Corrosion Protection of Steel in Concrete, Proceedings of International Conference, University of Sheffield, UK, 1994, p. 793.
[14] M.F. Montemor, A.M.P. Simoes, M.M. Salta, M.G.S. Ferreira, Carbonation of fly ash containing concrete—Electrochemical studies, in: Proceedings of the 12th International Corrosion Congress, Houston, Paper No. 76, 1993, NACE.
[15] M.F. Montemor, A.M.P. Simoes, M.G.S. Ferreira, Analytical characterization of the passive film formed on steel in solutions simulating the concrete interstitial electrolyte, Corrosion 54 (5) (1998) 347–353.
[16] M.F. Montemor, A.M.P. Simoes, M.M. Salta, Effect of fly ash on concrete reinforcement corrosion studied by EIS, Cem. Concr. Compos. 22 (2000) 175–185.
[17] K.M.A. Hossain, Effect of volcanic ash on cement based binder in concrete production, in: R. Dhir, T.D. Dyer (Eds.), Modern Concrete Materials: Binders, Additions and Admixtures, Thomas Telford, London, 1999, pp. 109–118.
[18] K.M.A. Hossain, B. Uy, Characteristics of volcanic ash and pumice based concrete, Proceedings of International Conference on Mechanics of Structures, Materials and Systems, February 17–19, University of Wollongong, Wollongong, Australia, 1999, pp. 239–244.
[19] K.M.A. Hossain, Properties of volcanic ash and pumice concrete, IABSE Rep. 80 (1999) 145–150.
[20] K.M.A. Hossain, Performance of volcanic ash concrete in marine environment, Proceedings of 24th OWICS Conference, 25–26 August, Singapore, 21st Century Concrete and Structures, vol. XVIII, CI Premier, 1999, pp. 209–214.
[21] M. Kawamura, K. Torii, Chloride permeability of concrete containing a fly ash and a blast furnace slag, Mater. Res. Soc. Symp. Proc. 137 (1989) 411–416.
[22] ASTM C618-91, Standard Specification for Fly Ash and Raw or Calcined Natural Pozzolan for Use as a Mineral Admixture in Portland Cement Concrete, Annual Book of ASTM Standards, Philadelphia, USA, 1991.
[23] O.E. Gjorv, Important test methods for evaluation of reinforced concrete durability, Concr. Technol. Past Present Future ACI SP-144 (1994) 545–574.
[24] L. Tang, L.-O. Nilsson, Rapid determination of chloride diffusivity in concrete by applying electrical field, ACI Mater. J. 89 (1) (1992) 49–53.
[25] J.Z. Zhang, N.R. Buenfeld, Development of the accelerated chloride migration test as a measure of chloride diffusivity in concrete, Corrosion and Corrosion Protection of Steel in Concrete, Proceedings of International Conference, University of Sheffield, vol. 1, 1994, pp. 395–403.
[26] Standard Method of Test for Rapid Determination of the Chloride Permeability of Concrete AASHTO T277-83, American Association of State Highway and Transportation Officials, Washington, DC, 1983.
[27] Japan Concrete Institute Standard: JCI-SC 5, Tokyo, Japan, 1994.
[28] J.P. Broomfield, P.E. Langford, A.J. Ewins, in: N.S. Berke, V. Chaker, D. Whiting (Eds.), Corrosion Rates of Steel in Concrete, ASTM STP 1065, Philadelphia, USA, 1990, p. 157.
[29] ASTM C876-91, Standard Test Method for Half-Cell Potentials of Uncoated Reinforcing Steel in Concrete, Annual Book of ASTM Standards, Philadelphia, USA, 1991.
[30] G. Ping, X. Ping, F. Yan, J.J. Beaudoin, Microstructural characterization of cementitious materials: Conductivity and impedance method, Materials Science of Concrete IV, American Ceramic Society, Westerville, OH, 1995, pp. 201–262.
[31] C.-L. Hwang, D.-H. Shen, The effects of blast-furnace slag and fly ash on the hydration of Portland cement, Cem. Concr. Res. 21 (4) (1991) 410–425.
[32] P.K. Brown, D.D. Shi, J. Skalny, Porosity/permeability relationships, in: J. Skalny, S. Mindess (Eds.), Materials Science of Concrete II, American Ceramic Society, Westerville, OH, 1991, pp. 83–109.
[33] N. Koulombi, G. Batis, C.H. Malami, in: J.M. Costa, A.D. Mercer (Eds.), Progress in the Understanding and Prevention of Corrosion, vol. 1, Institute of Materials, UK, 1993, p. 619.
[34] H.T. Cao, L. Bucea, D.E. McPhee, E.A. Christie, Corrosion of steel in solutions and cement pastes, corrosion of steel reinforcement in concrete, Final Report, Cement and Concrete Association of Australia, 1992.